JACS
JOURNAL OF THE AMERICAN CHEMICAL SOCIETY
Article
pubs.acs.org/JACS

Macrocyclization in the Design of Organic n-Type Electronic Materials

Melissa Ball,[†,§] Yu Zhong,[†,§] Brandon Fowler,[†] Boyuan Zhang,[†] Panpan Li,[†,‡] Grisha Etkin,[†] Daniel W. Paley,[†] John Decatur,[†] Ankur K. Dalsania,[†] Hexing Li,[‡] Shengxiong Xiao,*[,‡] Fay Ng,*[,†] Michael L. Steigerwald,*[,†] and Colin Nuckolls*[,†,‡]

[†]Department of Chemistry, Columbia University, New York, New York 10027, United States

[‡]The Education Ministry Key Lab of Resource Chemistry, Shanghai Key Laboratory of Rare Earth Functional Materials, Optoelectronic Nano Materials and Devices Institute, Department of Chemistry, Shanghai Normal University, Shanghai, China 200234

Supporting Information

ABSTRACT: Here, we compare analogous cyclic and acyclic π-conjugated molecules as n-type electronic materials and find that the cyclic molecules have numerous benefits in organic photovoltaics. This is the first report of such a direct comparison. We designed two conjugated cycles for this study. Each comprises four subunits: one combines four electron-accepting, redox-active, diphenyl-perylenediimide subunits, and the other alternates two electron-donating bithiophene units with two diphenyl-perylenediimide units. We compare the macrocycles to acyclic versions of these molecules and find that, relative to the acyclic analogs, the conjugated macrocycles have bathochromically shifted UV−vis absorbances and are more easily reduced. In blended films, macrocycle-based devices show higher electron mobility and good morphology. All of these factors contribute to the more than doubling of the power conversion efficiency observed in organic photovoltaic devices with these macrocycles as the n-type, electron transporting material. This study highlights the importance of geometric design in creating new molecular semiconductors. The ease with which we can design and tune the electronic properties of these cyclic structures charts a clear path to creating a new family of cyclic, conjugated molecules as electron transporting materials in optoelectronic and electronic devices.

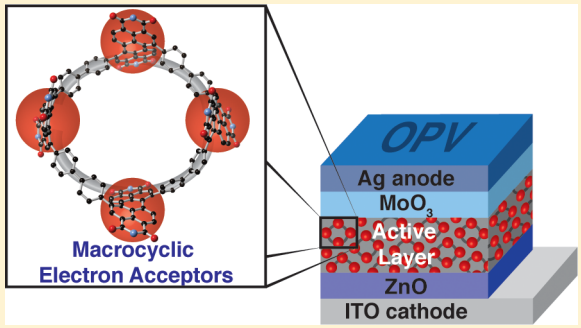

1. INTRODUCTION

We compare cyclic and acyclic π-conjugated molecules as n-type electronic materials and find that the cyclic molecules have numerous benefits in organic photovoltaics (OPVs). Conjugated macrocycles[1−27] have several potential advantages as organic electronic materials: (1) their contorted structure[28] should facilitate intermolecular contacts and charge transport; (2) they lack end groups that are known to create defects in linear polymers and act as trap-sites for charges as they move through materials;[29−33] (3) often they have an altered electronic structure;[1,7] and (4) they have a defined cavity that can be a host for electronically useful guest molecules.[6,22,34−36] Figure 1 displays the cyclic and acyclic molecules designed and synthesized for this study. The two conjugated cycles incorporate multiple repeat units of the redox-active, diphenyl-perylenediimide (**P**) subunit. One macrocycle alternates a bithiophene (**B**) unit with a **P** unit to form the **−P−B−P−B−** cyclic pattern, denoted here **cPBPB**, where "**c**" denotes cyclic. A second macrocycle (**c**$\mathbf{P_4}$) directly links the diphenyl-perylenediimide subunits into a tetrameric structure. We compare these macrocycles to a series of acyclic molecules (denoted with an "**a**" in Figure 1) that link varying numbers of **P** subunits and find that the conjugated cycles have bathochromically shifted UV−vis absorbances, are more easily reduced, have higher electron mobility, and better morphology in blended films. All of these factors contribute to the more than doubling of the power conversion efficiency (PCE) observed in solar cells using these macrocycles as n-type, electron-transporting material. This is the first report directly comparing analogous cyclic and acyclic π-conjugated molecules as n-type materials in OPVs.

2. RESULTS

Design. We designed a series of cyclic and acyclic π-conjugated molecules (Figure 1) that contain the redox active diphenyl-PDI subunit. PDIs possess many desirable properties such as efficient electron transport,[37−41] high molar absorptivities,[28,42,43] and ease of functionalization.[44−46] Derivatives of PDI are efficacious in solar cells when combined with electron-rich conjugated polymers.[43,47−49] We have developed a method to regioselectively create diaryl substituted versions of the PDI

Received: May 27, 2016
Published: September 26, 2016

DOI: 10.1021/jacs.6b05474
J. Am. Chem. Soc. 2016, 138, 12861−12867

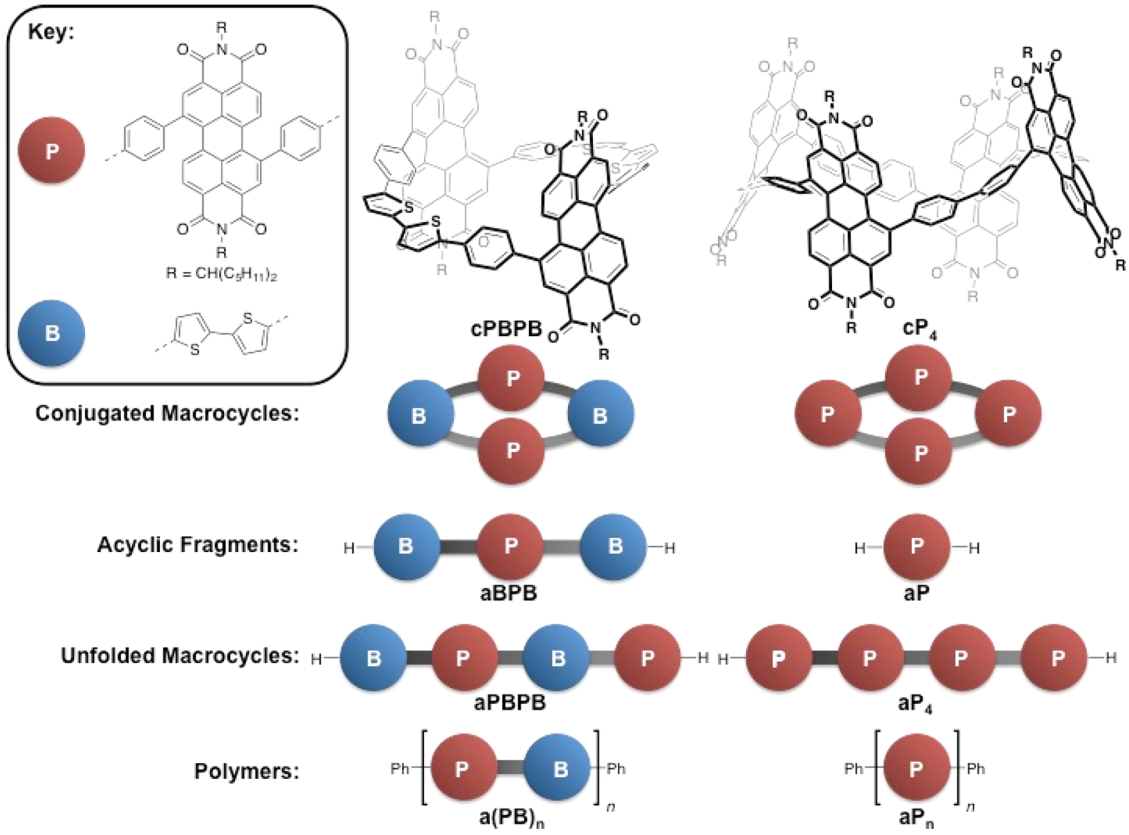

Figure 1. Structures of compounds designed and synthesized to compare as acyclic and cyclic, π-conjugated molecules for n-type electronic materials. We use the letter "**P**" to denote a diphenyl PDI and "**B**" for a bithiophene. Likewise, we use "**c**" and "**a**" for cyclic and acyclic, respectively.

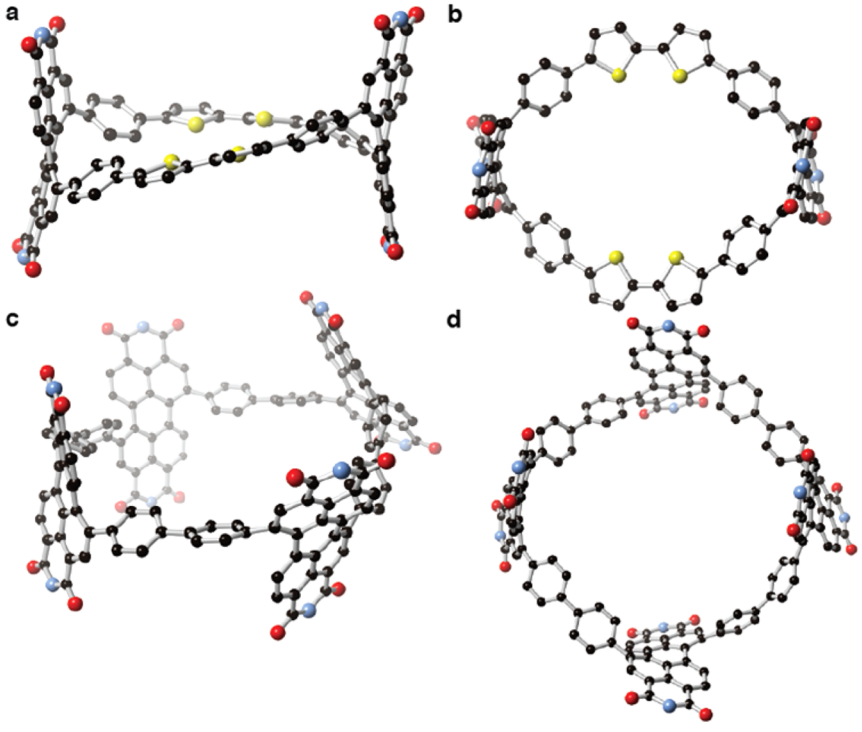

Figure 2. (a) Energy minimized structures from DFT for **cPBPB**. The (*S,S*)-stereoisomer is shown.[20] (b) Cavity view of **cPBPB**. (c) Energy minimized structures from DFT for **cP$_4$**. The (*S,S,S,S*)-stereoisomer is shown. (d) Cavity view for **cP$_4$**. Carbon = gray, nitrogen = blue, oxygen = red, and sulfur = yellow. Hydrogen atoms have been removed to clarify the view. A methyl group substitutes the side chains in the calculations. The methyl group, too, has been removed to clarify the view in the structures presented here.

DOI: 10.1021/jacs.6b05474
J. Am. Chem. Soc. 2016, 138, 12861−12867

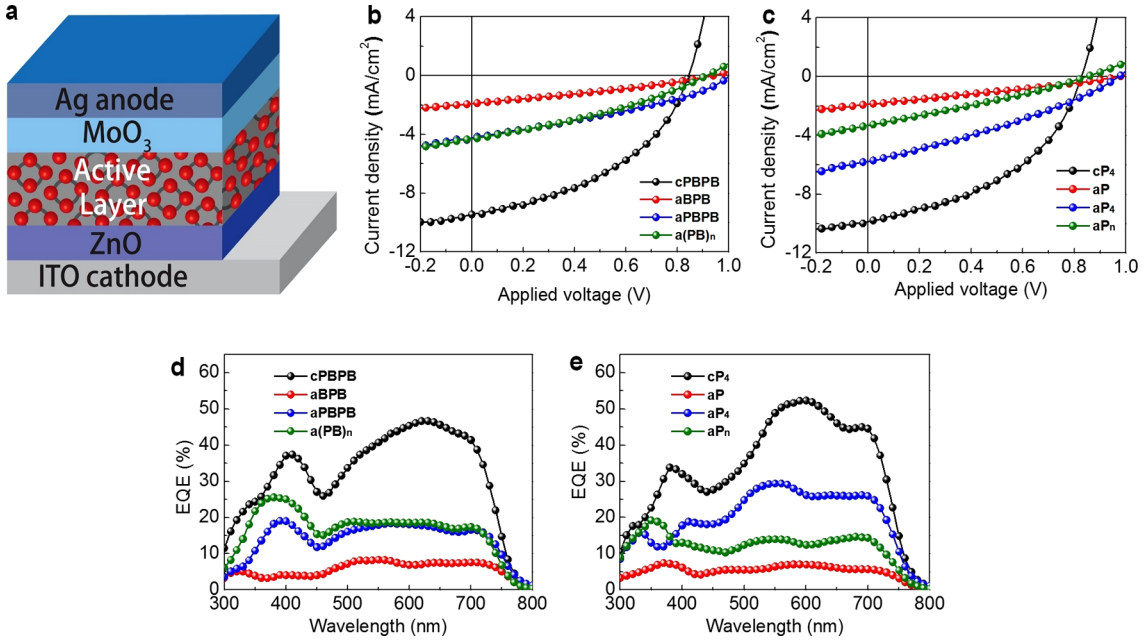

Figure 3. (a) Schematic of the solar cell device fabricated in this study. (b-e) *J*–*V* curves for (b) **cPBPB**-series and (c) **cP$_4$**-series solar cells under simulated AM 1.5G irradiation (100 mW cm^{-2}). EQE spectra for (d) **cPBPB** -series and (e) **cP$_4$**-series solar cells.

Table 1. Summary of Device Parameters of the Solar Cells Based on the Cycles and Acyclic Molecules[a]

	J_{sc} (mA cm^{-2})	V_{oc} (V)	FF	PCE (%)
cPBPB	9.2 ± 0.3	0.84 ± 0.01	0.44 ± 0.01	3.3 ± 0.2 (3.5)
aBPB	1.6 ± 0.2	0.94 ± 0.01	0.30 ± 0.01	0.46 ± 0.04 (0.53)
aPBPB	4.2 ± 0.1	1.00 ± 0.01	0.33 ± 0.01	1.3 ± 0.1 (1.4)
a(PB)$_n$	4.2 ± 0.2	0.90 ± 0.01	0.33 ± 0.01	1.1 ± 0.2 (1.3)
cP$_4$	9.7 ± 0.2	0.83 ± 0.01	0.44 ± 0.01	3.5 ± 0.1 (3.6)
aP	1.7 ± 0.1	0.97 ± 0.02	0.28 ± 0.01	0.46 ± 0.03 (0.51)
aP$_4$	5.8 ± 0.1	0.97 ± 0.01	0.32 ± 0.01	1.6 ± 0.2 (1.8)
aP$_n$	3.2 ± 0.1	0.85 ± 0.01	0.28 ± 0.01	0.73 ± 0.04 (0.78)

[a]Highest PCE values are shown in parentheses.

(see Supporting Information for details). From these diaryl substituted PDI subunits, we build the two macrocycles, **cPBPB** and **cP$_4$**, using a tetranucleur platinum macrocyclization followed by reductive eliminations.[4,7,14] The DFT minimized structures for **cPBPB**[20] and **cP$_4$** are shown in Figure 2.

For comparison to **cPBPB** and **cP$_4$**, we synthesized a series of acyclic molecules (also shown in Figure 1). The simplest structures are **aBPB** and **aP**; each possesses one **P** subunit. We also synthesized the precise analogs, "unfolded" macrocycles, that have one of their bonds cleaved and terminated with hydrogen atoms (**aPBPB** and **aP$_4$**). As a final point of comparison, we created the polymeric version of the macrocycles [**a(PB)$_n$** and **aP$_n$**]. The Supporting Information contains details of the synthesis and characterization of the cyclic and acyclic molecules used in this study.

OPVs. We fabricated devices from each of these macrocyclic and acyclic molecules. We chose the low-bandgap semiconducting polymer poly[4,8-bis(5-(2-ethylhexyl)thiophen-2-yl)benzo[1,2-*b*;4,5-*b*′]dithiophene-2,6-diyl-*alt*-(4-(2-ethylhexyl)-3-fluorothieno[3,4-*b*]thiophene)-2-carboxylate-2,6-diyl] (PTB7-Th)[50,51] as the electron-donating component in our devices. PTB7-Th is widely used as a high-performance donor material in both fullerene- and nonfullerene-based solar cells.[52,53] PTB7-Th is complementary to all molecules synthesized, as it absorbs more low-energy light (~550–800 nm). Figure S1 contains the film absorption spectra for all the compounds. We spin-cast the mixture of PTB7-Th and the cyclic or acyclic molecules to form a bulk heterojunction (BHJ) solar cell.[54] We used an inverted configuration of ITO/ZnO(20 nm)/PTB7-Th:acceptor/MoO_3(7 nm)/Ag(100 nm) for all of our solar cell devices.[55] A schematic of the device is shown in Figure 3a.

Figure 3b–e displays the OPV properties and the EQE measurements for each of the cyclic and acyclic molecules. Details for the optimization including varying the ratio of donor and acceptor, the additives, and the film thickness are included in the Supporting Information. The optimal active layers were ~100 nm in thickness. For the cyclic molecules, the optimal mass ratio was 1:2 for donor:acceptor. Furthermore, we optimized the films by using 1-chloronaphthalene (CN) as a solvent additive to control film morphology (Figure S4).[41] **cPBPB**'s PCE increases to 3.3% on average with a maximal value of 3.5%. Using an analogous procedure, we were able to achieve a PCE of 3.6% for **cP$_4$** (see Figure S3, Table S2, and Table 1). This is the first example of a macrocycle being used as the electron acceptor in an OPV.

Figure 3d,e shows the external quantum efficiency (EQE) curves for PTB7-Th:**cPBPB** and the PTB7-Th:**cP$_4$** solar cells. All the devices show broad photoresponse from 350 to 800 nm, consistent with the absorption spectra (Figure S1). Each EQE

DOI: 10.1021/jacs.6b05474
J. Am. Chem. Soc. 2016, 138, 12861–12867

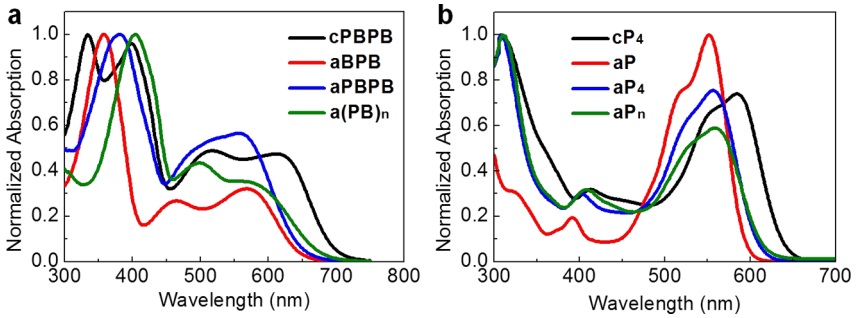

Figure 4. UV−vis absorption spectra measured in solution: (a) for **cPBPB**, **aBPB**, **aPBPB**, and **a(PB)**$_n$; (b) for **cP**$_4$, **aP**, **aP**$_4$, and **aP**$_n$ normalized to each absorption maxima, where absorption max = 1.

spectrum shows two transitions: a narrow band centered at ∼400 nm and a broad band centered at 620 nm for **cPBPB** and at 600 nm for **cP**$_4$. The EQE spectrum for **cP**$_4$ shows an increase relative to **cPBPB** at ∼700 nm. We note that both macrocycles show strong absorption from 400 to 650 nm (see Figure 4), indicating that photoexcitation in acceptor domains contributes to photocurrent in this type of solar cell. The integrated J_{sc} values are 9.2 and 9.8 mA cm^{-2} for PTB7-Th:**cPBPB** and the PTB7-Th:**cP**$_4$ solar cells, respectively. These values agree well with the measured J_{sc}, with a <3% mismatch. Upon addition of the CN additive, the EQE enhances over a broad range of wavelengths, particularly from 550 to 750 nm (Figures S2 and S3). Atomic force microscopy (AFM) of the films confirms that CN changes the film morphology, resulting in more efficient charge dissociation and transport (Figure S4). Like $PC_{71}BM$ and some nonfullerene acceptors,[47,52] complementary absorption between the macrocycles and the donor material is beneficial for harvesting light in the visible light region to maximize photocurrent.

We next compare the OPV results from the cyclic molecules to the acyclic molecules. Table 1 summarizes the device data. The key finding is that all of the acyclic molecules showed poor device performance on both an absolute and relative bases. Figure 3b,c displays the J−V curves for all the devices. We observe a couple of trends from this study: (1) smaller oligomer acyclic molecules (**aBPB**, **aPBPB**, **aP**, and **aP**$_4$) and the polymers [**a(PB)**$_n$ and **aP**$_n$] show decreased J_{sc} relative to the cyclic compounds; (2) the acyclic molecules also show higher V_{oc} values as compared to the cyclic acceptors; and (3) the acyclic molecules' poor PCEs are mainly attributed to the reduced J_{sc} and FFs relative to the cyclic ones. Figure 3d,e displays the comparison of external quantum spectra of the cyclics versus the acyclics. Overall, the photocurrent generation in cyclic-based devices is much larger than the acyclic-based devices. These results indicate that the cyclic acceptors have enhanced photocarrier generation and better charge transport.

To better understand the performance difference between the cyclic and acyclic molecules, we examined the electrochemistry, UV−vis absorption, electron mobility, and morphology of the films. These studies are described below.

Electrochemistry. We probe the variations in the frontier orbital energies for the macrocycles and their acyclic analogues using cyclic voltammetry (CV) (see Figure S5). The onset of the first oxidation and reduction peaks provides an estimate of the highest occupied molecular orbital (HOMO) and lowest unoccupied molecular orbital (LUMO) levels, respectively.[56] We find the acyclic molecules possess a more negative first reduction potential than the cyclic molecules. As a result, we observe higher energies for the LUMO for each of the acyclic molecules. The electrochemical data are summarized in Table 2.

Table 2. Comparison of the Band Gaps Estimated from CV and UV−vis Absorption Spectroscopy and OFET Performance

	electrochemical[a]			optical[b]	FET
	E_{LUMO} (eV)	E_{HOMO} (eV)	E_{gap} (eV)	E_{gap} (eV)	μ (cm^2 V^{-1} s^{-1})
cPBPB	−3.87	−5.39	1.52	2.02	(1.5 ± 0.2) × 10^{-3}
aBPB	−3.80	−5.42	1.62	2.18	(4.3 ± 0.2) × 10^{-4}
aPBPB	−3.80	−5.40	1.60	1.79	–
a(PB)$_n$	−3.86	−5.45	1.59	2.21	(2.3 ± 0.3) × 10^{-4}
cP$_4$	−3.90	−5.69	1.79	2.12	(1.5 ± 0.2) × 10^{-3}
aP	−3.75	–	–	2.25	(2.0 ± 0.3) × 10^{-5}
aP$_4$	−3.82	−5.77	1.95	2.23	–
aP$_n$	−3.86	−5.75	1.89	2.21	(1.9 ± 0.3) × 10^{-5}

[a]HOMO and LUMO levels were estimated from onset of the first oxidation and reduction peaks. [b]Optical band gaps were estimated from the wavelength at the absorption maximum.

The energy offset between the donor's HOMO and acceptor's LUMO is one of the factors that determines the V_{oc}s in BHJ solar cells.[57] The values obtained from CV results are in good agreement with the V_{oc} trend from the devices. Previous studies show a direct correlation between relatively large V_{oc} values coupled with low J_{sc} when the band offset does not provide sufficient driving force for exciton dissociation at the donor/acceptor interfaces.[58,59] Here, the observed trend suggests that the high LUMO levels, particularly in the short acyclic compounds, result in a higher occurrence of recombination and lower J_{sc}.[59,60]

Absorption Spectroscopy. Figure 4 compares the UV−vis absorption spectra of **cPBPB** and **cP**$_4$ to their acyclic counterparts. It is well documented that contorting linear molecules into cyclic structures significantly alters the electronic properties.[7,1] Absorptions in the cyclic compounds are bathochromically shifted relative to the linear, unstrained acyclic molecules. The CV data are also consistent with the UV−vis data. **cPBPB** and **cP**$_4$ have smaller HOMO−LUMO gaps relative to each of the corresponding acyclic molecules studied (Figure 4). Greater visible light absorption contributes to the more efficient solar cells for the cyclic molecules, providing the higher J_{sc} parameter for the cyclic molecules relative to the acyclic molecules.

Electron Mobility. Another factor that is critical for OPV device performance is electron transport through the acceptor phase. Poor carrier mobility impedes the carrier extraction and

DOI: 10.1021/jacs.6b05474
J. Am. Chem. Soc. 2016, 138, 12861−12867

results in increased carrier recombination inside OPV devices. This negatively impacts the J_{sc}, FF, and overall solar cell performance. To investigate the electron mobility of these compounds, we fabricated organic field-effect transistors (OFETs). The Supporting Information describes the preparation of the devices and the methodology used to extract the OFET characteristics. All molecules measured form n-type, electron-transporting thin-film semiconductors.[37,61] Figure 5

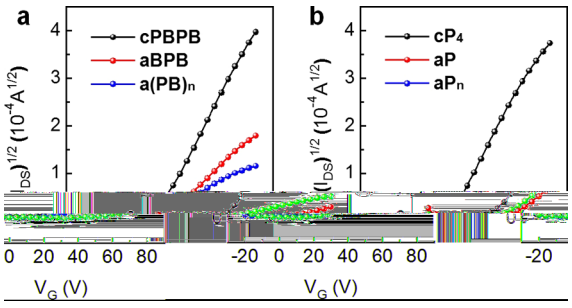

Figure 5. OFET transfer characteristics plotted in $(I_{DS})^{1/2}-V_G$ axes for (a) **cPBPB**, **aBPB**, and **a(PB)**$_n$; (b) for **cP**$_4$, **aP**, and **aP**$_n$. The V_{DS} is 80 V.

displays typical transfer curves in the saturation regime. The mobility was calculated in the saturation regime using $I_{DS} = (W/2L)C_i\mu(V_G - V_T)$,[2] where W and L are the width and length of the channel, C_i (11.5 nFcm^{-2}), μ, and V_T correspond to the capacitance per unit area of the gate insulator, the field effect mobility, and the threshold voltage, respectively.[62] Both **cPBPB** and **cP**$_4$ show electron mobility of $(1.5 \pm 0.2) \times 10^{-3}$ cm^2 V^{-1}s $^{-1}$. One of the key findings is the cyclic molecules have a far greater ability to transport electrons in thin-film devices relative to the acyclic molecules. Table 2 shows electron mobility for six of the compounds studied. **cPBPB**'s average mobility is 5-fold higher than its acyclic counterparts; **cP**$_4$'s mobility is nearly 2 orders of magnitude higher than its counterparts. The cyclic structures far greater ability to transport electrons contributes to the overall better solar cell performance.

Morphology. At the nanoscale level, phase separation between the donor and the acceptor plays an important role in providing an efficient donor/acceptor interface and a continuous pathway for carrier transport. Appropriate aggregation and phase separation are critical to device performance of BHJs in terms of charge dissociation and carrier transport. We performed AFM to study the surface morphology of the active layers. Figure 6 displays phase images of the six active layers studied. The corresponding height images are displayed in Figure S6. For both **cPBPB** and **cP**$_4$, the active layers possess clear phase separation as shown in Figure 6a,d. The average domain size is estimated to be 20−40 nm. For the polymeric **a(PB)**$_n$ and **aP**$_n$, the domain sizes are relatively small (10−30 nm). It is difficult to detect efficient phase segregation in these films. The active layers containing **aBPB** and **aP** have large domain sizes; they are in the range of 50−70 nm, as shown in Figure 6b,e. These features exceed twice the typical exciton diffusion length (ca. 10−20 nm) in organic semiconductors. Thus, photogenerated excitons within the domain recombine before they reach the donor/acceptor interface.[54,63] The overaggregation in the **aBPB** and **aP** solar cells likely results in carrier recombination and poor device performance. In the **cPBPB**- and **cP**$_4$-based BHJ systems, phase aggregation is essential to the device performance as it enables an efficient donor/acceptor interface and a 3D continuous pathway for efficient carrier transport.

3. CONCLUSION

This is the first study comparing cyclic structures to their acyclic counterparts in OPVs. We found that the cyclic structures far outperform the acyclic controls in organic photovoltaics. We find it interesting that **cPBPB** and **cP**$_4$ perform similarly as the electron transporting material in OPVs even though **cPBPB** has a bathochromically shifted UV−vis compared to that of **cP**$_4$. The origin of the increase in the efficiency of the devices when cyclic molecules are used in place of acyclic ones is multifaceted. When compared to the acyclic

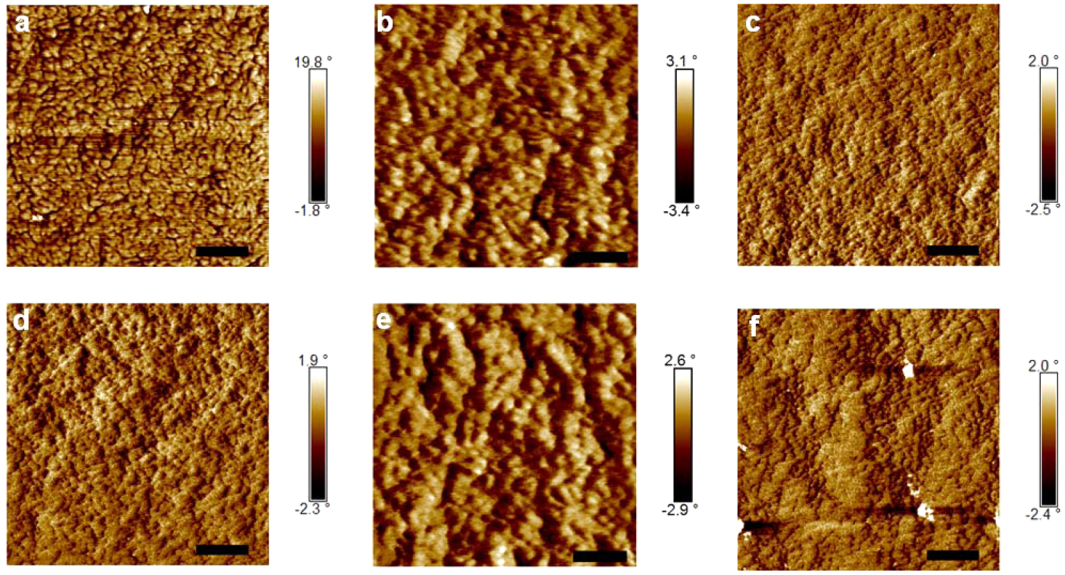

Figure 6. AFM phase images of bulkjunction films for (a) **cPBPB**, (b) **aBPB**, (c) **a(PB)**$_n$, (d) **cP**$_4$, (e) **aP**, and (f) **aP**$_n$. The mass ratio of donor-to-acceptor is fixed at 1:2. 1% CN additive was used. The scale bar is 200 nm.

DOI: 10.1021/jacs.6b05474
J. Am. Chem. Soc. 2016, 138, 12861−12867

molecules, the macrocycles: (1) have better energy alignment with the donor material; (2) absorb more visible light; (3) are more efficient at transporting electrons; and (4) show optimal phase separation for BHJ solar cells. The ease with which we can tune the energetics and therefore the properties of these macrocycles—through a different linker subunit or incorporating oligomeric PDI subunits—will magnify these initial findings.[53] This study also offers the intriguing possibility of tuning the geometry of the donor so that it is shape matched to these cyclic electron-accepting structures as a means to creating highly efficient devices.

■ ASSOCIATED CONTENT

Supporting Information

The Supporting Information is available free of charge on the ACS Publications website at DOI: 10.1021/jacs.6b05474.

Experimental procedures for the synthesis and characterization of **aBPB**, **aPBPB**, **a(PB)$_n$**, **cP$_4$**, **aP**, **aP$_4$**, and **aP$_n$**. UV−vis spectroscopy, cyclic voltammetry, field effect transistor and solar cell device fabrication, characterization methods, device performance, AFM images, and computational details (PDF)

■ AUTHOR INFORMATION

Corresponding Authors

*senksong@msn.com
*fwn2@columbia.edu
*mls2064@columbia.edu
*cn37@columbia.edu

Author Contributions

§These authors contributed equally.

Notes

The authors declare no competing financial interest.

■ ACKNOWLEDGMENTS

Primary support for this project was provided by the Chemical Sciences, Geosciences and Biosciences Division, Office of Basic Energy Sciences, U.S. Department of Energy (DOE), under award no. DE-FG02-01ER15264. The Columbia University Shared Materials Characterization Laboratory (SMCL) was used extensively for this research. We are grateful to Columbia University for support of this facility. S.X., H.L., and P.L. were sponsored by National Natural Science Foundation of China (no. 21473113), Program for Professor of Special Appointment (Eastern Scholar) at Shanghai Institutions of Higher Learning (no. 2013-57), "Shuguang Program" supported by Shanghai Education Development Foundation and Shanghai Municipal Education Commission (no. 14SG40), Program of Shanghai Academic Research Leader (no. 16XD1402700), Program for Changjiang Scholars and Innovative Research Team in University (IRT1269), and International Joint Laboratory on Resource Chemistry (IJLRC).

■ REFERENCES

(1) Krömer, J.; Rios-Carreras, I.; Fuhrmann, G.; Musch, C.; Wunderlin, M.; Debaerdemaeker, T.; Mena-Osteritz, E.; Bäuerle, P. *Angew. Chem., Int. Ed.* **2000**, *39*, 3481.
(2) Nakao, K.; Nishimura, M.; Tamachi, T.; Kuwatani, Y.; Miyasaka, H.; Nishinaga, T.; Iyoda, M. *J. Am. Chem. Soc.* **2006**, *128*, 16740.
(3) Jasti, R.; Bhattacharjee, J.; Neaton, J. B.; Bertozzi, C. R. *J. Am. Chem. Soc.* **2008**, *130*, 17646.
(4) Zhang, F.; Gotz, G.; Winkler, H. D. F.; Schalley, C. A.; Bauerle, P. *Angew. Chem., Int. Ed.* **2009**, *48*, 6632.
(5) Omachi, H.; Matsuura, S.; Segawa, Y.; Itami, K. *Angew. Chem., Int. Ed.* **2010**, *49*, 10202.
(6) Iwamoto, T.; Watanabe, Y.; Sadahiro, T.; Haino, T.; Yamago, S. *Angew. Chem., Int. Ed.* **2011**, *50*, 8342.
(7) Iwamoto, T.; Watanabe, Y.; Sakamoto, Y.; Suzuki, T.; Yamago, S. *J. Am. Chem. Soc.* **2011**, *133*, 8354.
(8) Segawa, Y.; Miyamoto, S.; Omachi, H.; Matsuura, S.; Senel, P.; Sasamori, T.; Tokitoh, N.; Itami, K. *Angew. Chem., Int. Ed.* **2011**, *50*, 3244.
(9) Segawa, Y.; Senel, P.; Matsuura, S.; Omachi, H.; Itami, K. *Chem. Lett.* **2011**, *40*, 423.
(10) Sprafke, J. K.; Kondratuk, D. V.; Wykes, M.; Thompson, A. L.; Hoffmann, M.; Drevinskas, R.; Chen, W.-H.; Yong, C. K.; Kärnbratt, J.; Bullock, J. E.; Malfois, M.; Wasielewski, M. R.; Albinsson, B.; Herz, L. M.; Zigmantas, D.; Beljonne, D.; Anderson, H. L. *J. Am. Chem. Soc.* **2011**, *133*, 17262.
(11) Hitosugi, S.; Nakanishi, W.; Isobe, H. *Chem. - Asian J.* **2012**, *7*, 1550.
(12) Hitosugi, S.; Yamasaki, T.; Isobe, H. *J. Am. Chem. Soc.* **2012**, *134*, 12442.
(13) Ishii, Y.; Nakanishi, Y.; Omachi, H.; Matsuura, S.; Matsui, K.; Shinohara, H.; Segawa, Y.; Itami, K. *Chem. Sci.* **2012**, *3*, 2340.
(14) Kayahara, E.; Sakamoto, Y.; Suzuki, T.; Yamago, S. *Org. Lett.* **2012**, *14*, 3284.
(15) Omachi, H.; Segawa, Y.; Itami, K. *Acc. Chem. Res.* **2012**, *45*, 1378.
(16) Evans, P. J.; Darzi, E. R.; Jasti, R. *Nat. Chem.* **2014**, *6*, 404.
(17) Kayahara, E.; Patel, V. K.; Yamago, S. *J. Am. Chem. Soc.* **2014**, *136*, 2284.
(18) Yamago, S.; Kayahara, E.; Iwamoto, T. *Chem. Rec.* **2014**, *14*, 84.
(19) Asai, K.; Fukazawa, A.; Yamaguchi, S. *Chem. Commun.* **2015**, *51*, 6096.
(20) Ball, M.; Fowler, B.; Li, P.; Joyce, L. A.; Li, F.; Liu, T.; Paley, D.; Zhong, Y.; Li, H.; Xiao, S.; Ng, F.; Steigerwald, M. L.; Nuckolls, C. *J. Am. Chem. Soc.* **2015**, *137*, 9982.
(21) Chang, S.-W.; Horie, M. *Chem. Commun.* **2015**, *51*, 9113.
(22) Chen, Q.; Trinh, M. T.; Paley, D. W.; Preefer, M. B.; Zhu, H.; Fowler, B. S.; Zhu, X.-Y.; Steigerwald, M. L.; Nuckolls, C. *J. Am. Chem. Soc.* **2015**, *137*, 12282.
(23) Darzi, E. R.; Hirst, E. S.; Weber, C. D.; Zakharov, L. N.; Lonergan, M. C.; Jasti, R. *ACS Cent. Sci.* **2015**, *1*, 335.
(24) Ito, H.; Mitamura, Y.; Segawa, Y.; Itami, K. *Angew. Chem., Int. Ed.* **2015**, *54*, 159.
(25) Jiang, H.-W.; Tanaka, T.; Mori, H.; Park, K. H.; Kim, D.; Osuka, A. *J. Am. Chem. Soc.* **2015**, *137*, 2219.
(26) Kuwabara, T.; Orii, J.; Segawa, Y.; Itami, K. *Angew. Chem., Int. Ed.* **2015**, *54*, 9646.
(27) Van Raden, J. M.; Darzi, E. R.; Zakharov, L. N.; Jasti, R. *Org. Biomol. Chem.* **2016**, *14*, 5721.
(28) Ball, M.; Zhong, Y.; Wu, Y.; Schenck, C.; Ng, F.; Steigerwald, M.; Xiao, S. X.; Nuckolls, C. *Acc. Chem. Res.* **2015**, *48*, 267.
(29) Nicolai, H. T.; Kuik, M.; Wetzelaer, G. A. H.; de Boer, B.; Campbell, C.; Risko, C.; Brédas, J. L.; Blom, P. W. M. *Nat. Mater.* **2012**, *11*, 882.
(30) Mandoc, M. M.; de Boer, B.; Paasch, G.; Blom, P. W. M. *Phys. Rev. B: Condens. Matter Mater. Phys.* **2007**, *75*, 193202.
(31) Arias, A. C.; MacKenzie, J. D.; McCulloch, I.; Rivnay, J.; Salleo, A. *Chem. Rev.* **2010**, *110*, 3.
(32) Kaake, L. G.; Barbara, P. F.; Zhu, X.-Y. *J. Phys. Chem. Lett.* **2010**, *1*, 628.
(33) Sirringhaus, H. *Adv. Mater.* **2005**, *17*, 2411.
(34) Iyoda, M.; Yamakawa, J.; Rahman, M. J. *Angew. Chem., Int. Ed.* **2011**, *50*, 10522.
(35) Iwamoto, T.; Watanabe, Y.; Takaya, H.; Haino, T.; Yasuda, N.; Yamago, S. *Chem. - Eur. J.* **2013**, *19*, 14061.

DOI: 10.1021/jacs.6b05474
J. Am. Chem. Soc. 2016, 138, 12861−12867

(36) Nakanishi, Y.; Omachi, H.; Matsuura, S.; Miyata, Y.; Kitaura, R.; Segawa, Y.; Itami, K.; Shinohara, H. *Angew. Chem., Int. Ed.* **2014**, *53*, 3102.
(37) Anthony, J. E.; Facchetti, A.; Heeney, M.; Marder, S. R.; Zhan, X. W. *Adv. Mater.* **2010**, *22*, 3876.
(38) Zhou, E. J.; Cong, J. Z.; Wei, Q. S.; Tajima, K.; Yang, C. H.; Hashimoto, K. *Angew. Chem., Int. Ed.* **2011**, *50*, 2799.
(39) Li, C.; Wonneberger, H. *Adv. Mater.* **2012**, *24*, 613.
(40) Sharenko, A.; Proctor, C. M.; van der Poll, T. S.; Henson, Z. B.; Nguyen, T. Q.; Bazan, G. C. *Adv. Mater.* **2013**, *25*, 4403.
(41) Cai, Y.; Huo, L.; Sun, X.; Wei, D.; Tang, M.; Sun, Y. *Adv. Energy Mater.* **2015**, *5*, 1500032.
(42) Nolde, F.; Pisula, W.; Muller, S.; Kohl, C.; Mullen, K. *Chem. Mater.* **2006**, *18*, 3715.
(43) Zhong, Y.; Kumar, B.; Oh, S.; Trinh, M. T.; Wu, Y.; Elbert, K.; Li, P. P.; Zhu, X. Y.; Xiao, S. X.; Ng, F.; Steigerwald, M. L.; Nuckolls, C. *J. Am. Chem. Soc.* **2014**, *136*, 8122.
(44) Yan, Q. F.; Zhao, D. H. *Org. Lett.* **2009**, *11*, 3426.
(45) Huo, L. J.; Zhou, Y.; Li, Y. F. *Macromol. Rapid Commun.* **2008**, *29*, 1444.
(46) Würthner, F.; Saha-Möller, C. R.; Fimmel, B.; Ogi, S.; Leowanawat, P.; Schmidt, D. *Chem. Rev.* **2016**, *116*, 962.
(47) Zhong, Y.; Trinh, M. T.; Chen, R. S.; Wang, W.; Khlyabich, P. P.; Kumar, B.; Xu, Q. Z.; Nam, C. Y.; Sfeir, M. Y.; Black, C.; Steigerwald, M. L.; Loo, Y. L.; Xiao, S. X.; Ng, F.; Zhu, X. Y.; Nuckolls, C. *J. Am. Chem. Soc.* **2014**, *136*, 15215.
(48) Meng, D.; Sun, D.; Zhong, C.; Liu, T.; Fan, B.; Huo, L.; Li, Y.; Jiang, W.; Choi, H.; Kim, T.; Kim, J. Y.; Sun, Y.; Wang, Z.; Heeger, A. J. *J. Am. Chem. Soc.* **2016**, *138*, 375.
(49) Wu, Q.; Zhao, D.; Schneider, A. M.; Chen, W.; Yu, L. *J. Am. Chem. Soc.* **2016**, *138*, 7248.
(50) Liang, Y.; Xu, Z.; Xia, J.; Tsai, S.-T.; Wu, Y.; Li, G.; Ray, C.; Yu, L. *Adv. Mater.* **2010**, *22*, E135.
(51) Liao, S.-H.; Jhuo, H.-J.; Cheng, Y.-S.; Chen, S.-A. *Adv. Mater.* **2013**, *25*, 4766.
(52) He, Z.; Xiao, B.; Liu, F.; Wu, H.; Yang, Y.; Xiao, S.; Wang, C.; Russell, T. P.; Cao, Y. *Nat. Photonics* **2015**, *9*, 174.
(53) Zhong, Y.; Trinh, M. T.; Chen, R.; Purdum, G. E.; Khlyabich, P. P.; Sezen, M.; Oh, S.; Zhu, H.; Fowler, B.; Zhang, B.; Wang, W.; Nam, C.-Y.; Sfeir, M. Y.; Black, C. T.; Steigerwald, M. L.; Loo, Y.-L.; Ng, F.; Zhu, X.-Y.; Nuckolls, C. *Nat. Commun.* **2015**, *6*, 8242.
(54) Heeger, A. J. *Adv. Mater.* **2014**, *26*, 10.
(55) Sun, Y.; Seo, J. H.; Takacs, C. J.; Seifter, J.; Heeger, A. J. *Adv. Mater.* **2011**, *23*, 1679.
(56) You, J. B.; Dou, L. T.; Yoshimura, K.; Kato, T.; Ohya, K.; Moriarty, T.; Emery, K.; Chen, C. C.; Gao, J.; Li, G.; Yang, Y. *Nat. Commun.* **2013**, *4*, 1446.
(57) Elumalai, N. K.; Uddin, A. *Energy Environ. Sci.* **2016**, *9*, 391.
(58) Wang, M.; Wang, H.; Yokoyama, T.; Liu, X.; Huang, Y.; Zhang, Y.; Nguyen, T.-Q.; Aramaki, S.; Bazan, G. C. *J. Am. Chem. Soc.* **2014**, *136*, 12576.
(59) Li, W.; Hendriks, K. H.; Furlan, A.; Wienk, M. M.; Janssen, R. A. J. *J. Am. Chem. Soc.* **2015**, *137*, 2231.
(60) Hendriks, K. H.; Wijpkema, A. S. G.; van Franeker, J. J.; Wienk, M. M.; Janssen, R. A. J. *J. Am. Chem. Soc.* **2016**, *138*, 10026.
(61) Zhao, Y.; Guo, Y.; Liu, Y. *Adv. Mater.* **2013**, *25*, 5372.
(62) Newman, C. R.; Frisbie, C. D.; Filho; da, S.; Brédas, J.-L.; Ewbank, P. C.; Mann, K. R. *Chem. Mater.* **2004**, *16*, 4436.
(63) Dou, L.; You, J.; Hong, Z.; Xu, Z.; Li, G.; Street, R. A.; Yang, Y. *Adv. Mater.* **2013**, *25*, 6642.

DOI: 10.1021/jacs.6b05474
J. Am. Chem. Soc. 2016, 138, 12861−12867